Received: 27 June 2020 | Revised: 13 August 2020 | Accepted: 18 August 2020

DOI: 10.1111/ffe.13339

ORIGINAL CONTRIBUTION

FFEMS Fatigue & Fracture of Engineering Materials & Structures WILEY

Experimental investigation on the influence of welding residual stresses on fatigue for two different weld geometries

Nils Friedrich

Institute for Ship Structural Design and Analysis, Hamburg University of Technology, Hamburg, Germany

Correspondence
Nils Friedrich, Hamburg University of Technology, Institute for Ship Structural Design and Analysis, Am Schwarzenberg-Campus 4 C, 21073 Hamburg, Germany.
Email: nils.friedrich@tuhh.de

Abstract

Fatigue tests on welded small-scale specimens often do not show a distinct residual stress influence. An exception is longitudinal stiffeners, which are therefore frequently used to study the influence of welding residual stresses on fatigue. The results are not directly transferable to other weld geometries because the residual stress distribution depends on the weld geometries. In the presented investigation, fatigue tests on multilayer K-butt weld and longitudinal stiffener specimens were performed. The tests were carried out in the as-welded and stress-relieved conditions at different load ratios. Initiation of macroscopic cracks was detected using digital image correlation. This allowed determining the influence of welding residual stresses on the initiation of macroscopic cracks, crack propagation and total fatigue life for both investigated weld geometries.

KEYWORDS

crack propagation, digital image correlation, initiation of macroscopic cracks, longitudinal stiffener, multilayer K-butt weld, stress ratio

1 | INTRODUCTION

As welding residual stresses are superimposed to fatigue loads, they affect the stress ratio. In the case of tensile residual stresses, the actual stress ratio is shifted towards tension. Depending on the level of the residual stresses and the applied stress range, the actual stress ratio will be the same independently of the applied load ratio.[1] Thus, the influence of the applied stress ratio on the fatigue strength is diminished in presence of residual stresses.

Although this qualitative principle is long known, a quantitative assessment of the residual stress influence on fatigue is still challenging. One difficulty is the determination of the residual stresses. Measurements and simulation procedures are relatively complex, yet results are often not unambiguous. Another difficulty regards experimental investigations. Welded small-scale specimens often do not show a distinct residual stress influence on fatigue.

This applies in particular to specimens with welds transversal to the loading direction. According to Nitschke-Pagel,[2] on transversal welds, the highest (transversal) residual stresses occur in the middle of the weld, not at the weld toe critical for fatigue cracks. They will have a noticeable influence on fatigue strength only in particular cases, for example, high strength steels. These results are based on small-scale specimens. Different mean stress sensitivities for small-scale and structure-

like specimens on butt welds and transversal stiffeners due to lower residual stresses in small specimens were found in Buxbaum.[3]

An exception is formed by longitudinal stiffeners on which the weld is constrained by the specimen itself. Therefore, this specimen type is often used to investigate the influence of welding residual stresses on fatigue. However, also for this weld, geometry results are not always concordant. In Varfolomeev et al[4] and Siegele et al,[5] numerical and experimental investigations showed a reduced residual stress influence on longitudinal stiffeners. This was explained by the decrease of transversal residual stresses in proximity of the weld and residual stress relaxation after the first load cycles. In Hensel et al,[6] tests on straightened specimens showed an influence also for longitudinal stiffeners, leading to the conclusion that welding distortion may have covered residual stress effects in some previous studies.

The residual stress influence on fatigue will also depend on the applied load. When relatively high stresses occur, for example, due to high tensile loads in the low-cycle regime, plastic strains may lead to a reduction of tensile residual stresses and thus of their influence on fatigue.[7] High stresses affecting residual stresses and their influence on fatigue may occur also due to the stress concentration at a notch.[8] The influence of tensile residual stresses will therefore be more evident for load cases with compressive or low tensile loads and vanish for high tensile loads.

Residual stress distributions vary between weld geometries but also over the cross section of the specimen. Over the plate thickness residual stresses may vary between tensile and compressive values.[9] Apart from the residual stress level at the surface, which will affect crack initiation, crack propagation will be influenced by the residual stress state at the tip of the crack. Therefore, also the residual stress distribution over the thickness will affect their influence on fatigue strength. In Chattopadhyay et al,[10] numerical investigations on the crack initiation and crack propagation considering residual stresses at a tubular joint with the weld geometry similar to a longitudinal stiffener have been performed. In presence of residual stresses, the part of crack initiation in total fatigue life was approximately doubled. In Rörup,[11] the influence under compressive pulsating stresses has been investigated for longitudinal stiffeners. Crack initiation under compressive loading has been explained by tensile residual stresses at the weld. Compressive residual stresses have been shown to slow down crack propagation in Tateishi et al.[12] Recently, crack propagation under the influence of residual stresses has been studied in numerical and experimental investigations on brazed pipe specimens[13] and friction stir welded specimens.[14]

Thus, the residual stress influence on fatigue is expected to depend on the weld geometry and to vary for crack initiation and propagation depending on the residual stress distribution over the cross-section. Therefore, in this paper, experimental investigations on two weld geometries are presented including the detection of the initiation of macroscopic cracks. Fatigue tests are performed on specimens with a multilayer K-butt weld and longitudinal stiffeners to compare the results for specimens with a transversal weld and a longitudinal stiffener. The tests are performed at different load ratios in the as-welded and stress-relieved condition to determine the influence of welding residual stresses. The initiation of macroscopic cracks is detected using digital image correlation (DIC), in order to compare the influence on crack initiation, propagation and total fatigue life.

2 | TEST SPECIMENS

2.1 | Specimen preparation

Two sets of test specimens are prepared with two different weld geometries, a multilayer K-butt weld and a longitudinal stiffener (Figure 1). All specimens have a cross-section of 55 × 10 mm and a length of 500 mm. The K-butt weld specimens are made of S355J2C + N steel with a yield strength of R_{eH} = 394 MPa determined in tensile tests at room temperature and the longitudinal stiffener specimens of S355J2 + N with $R_{p0.2}$ = 370 MPa. The K-butt weld specimens are cut from the welded plates after cooling to room temperature using a band saw. With the welding sequence shown in (Figure 1A), tensile residual stresses at the weld toe of the K-butt weld are obtained. The longitudinal stiffeners are welded with a single layer fillet weld. Welding is performed by hand using metal active gas for both specimen types. During welding, the plates are tack welded to steel profiles to reduce welding distortion. The profiles are removed after the specimens have cooled to room temperature. Two-thirds of the specimens are thermally stress-relieved so that their fatigue behaviour is not influenced by residual stresses. In the following fatigue tests, half of these specimens is used as comparison to evidence the residual stress influence in the as-welded specimens. The rest of the stress-relieved specimens is used in another test series, which is not part of this paper. Additional information on the specimen preparation can be found in Friedrich and Ehlers.[15,16]

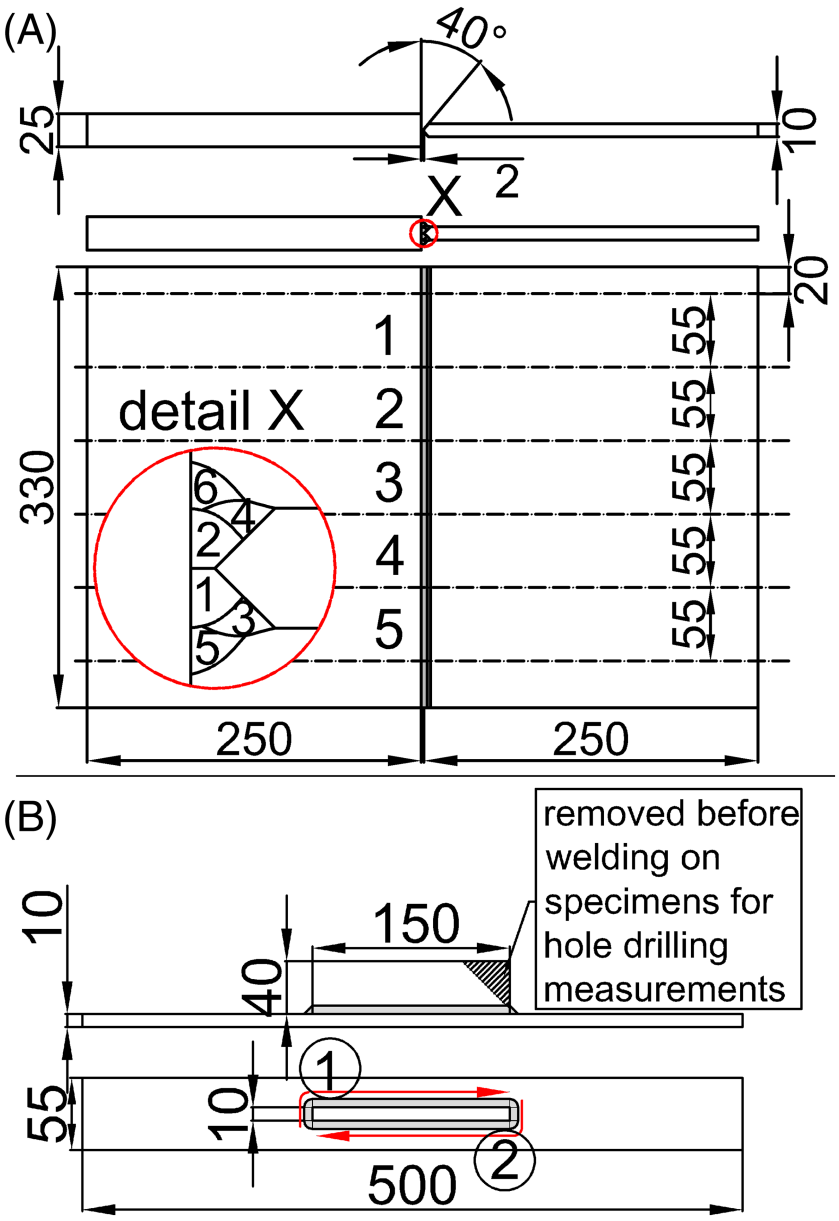

FIGURE 1 A, K-butt weld specimen preparation and welding sequence. B, longitudinal stiffener specimen and welding sequence indicated by ① and ② [Colour figure can be viewed at wileyonlinelibrary.com]

2.1.1 | Specimen distortion

When clamping a distorted specimen in the testing machine, the distortion will result in a bending moment and thus bending stresses. These will be added to the applied load stress and therefore affect the effective stress ratio. As also the residual stresses affect the effective stress ratio with excessive clamping stresses, the effect of residual stresses will not be recognisable. Furthermore, welding distortions and residual stresses are closely related. Processes that change residual stresses can also result in changes of distortions. Half of the specimens used in the fatigue tests is thermally stress-relieved. In this process, the specimens are heated, and residual stresses are relieved as they exceed the reduced yield limit at elevated temperatures.[17] This will cause plastic strains in the material as a new equilibrium between residual stresses at the lowered yield limit is established. The heat treatment may cause additional distortions in the specimens. To determine the residual stress influence, it is important that distortions are similar for the as-welded and the stress-relieved specimens.

The distortion of the K-butt weld specimens is determined by measuring the height difference between four points, two on each side of the weld, compare with.[18]

The calculated mean values of misalignment and distortion on the K-butt weld specimens are given in Table 1. The differences lie within the measurement accuracy. Some specimens are measured before and after stress-relieve treatment. No change of the measured distortion is found.

Also on the longitudinal stiffeners, the distortion is determined by measuring the height difference between four points on the specimen. For the longitudinal stiffener, the results are only qualitative. The specimens have an angular distortion at both ends of the stiffener. Because of minor differences in the specimens' lengths, it is difficult to position the centre of the stiffener accurately between the measuring points.

The calculated mean values of the angular distortion and the deflection at the centre of the specimen with respect to its ends are given in Table 1. The distortion increases slightly after stress-relieving. This is in line with findings in Fricke and Tchuindjang,[19] where the deflections were between 0 and 1 mm in the as-welded condition and up to 8 mm after stress-relieving on longitudinal stiffener specimens of 600 mm length. In Hensel et al,[6] angular distortions of more than 1.0° were corrected mechanically to between 0.09° and 0.15°.

Although the performed measurements are not accurate, they allow a qualitative assessment of the welding distortions. Compared with distortion values found in literature, the measured values appear to be on the lower side. For the K-butt weld, no difference between as-welded and stress-relieved specimens was found. For the longitudinal stiffeners, the distortion increased slightly after stress-relieve treatment. In the following fatigue test, levelling plates will be used to compensate the distortions. Thus, it will not be possible to calculate the clamping stresses or secondary bending stresses analytically, and the measurements are used only for verification purposes. The distortion measurements are therefore not repeated by more adequate means (e.g., laser scanner).

TABLE 1 Mean values of distortion

K-butt weld		
	As-welded	**Stress-relieved**
Angular distortion	0.33°	0.35°
Standard deviation	0.16°	0.12°
Linear misalignment	0.33 mm	0.47 mm
Standard deviation	0.45 mm	0.29 mm
Longitudinal stiffener		
	As-welded	Stress-relieved
Angular distortion	0.38°	0.47°
Standard deviation	0.21°	0.25°
Deflection	0.58 mm	0.72 mm
Standard deviation	0.27 mm	0.28 mm

2.2 | Residual stress measurements

Residual stresses are measured using two different measuring techniques: X-ray diffraction and hole-drilling. On the K-butt weld specimens, the measurements are performed on the 10-mm-thick plate. On the longitudinal stiffener specimens, residual stresses are measured in front of the boxing weld at the right end of the stiffener, referred to Figure 1B. The resulting residual stresses transversal to the weld, this corresponds to the loading direction of the specimens, are plotted in Figure 2 for both specimen geometries. Numerical simulations presented in Friedrich and Ehlers[15] show that after cutting the K-butt weld plates, the resulting specimens present a similar residual stress distribution as the original plates with compressive transversal residual stresses at the edges and tensile values in the centre. The residual stresses are caused mainly by the shrinkage of the weld

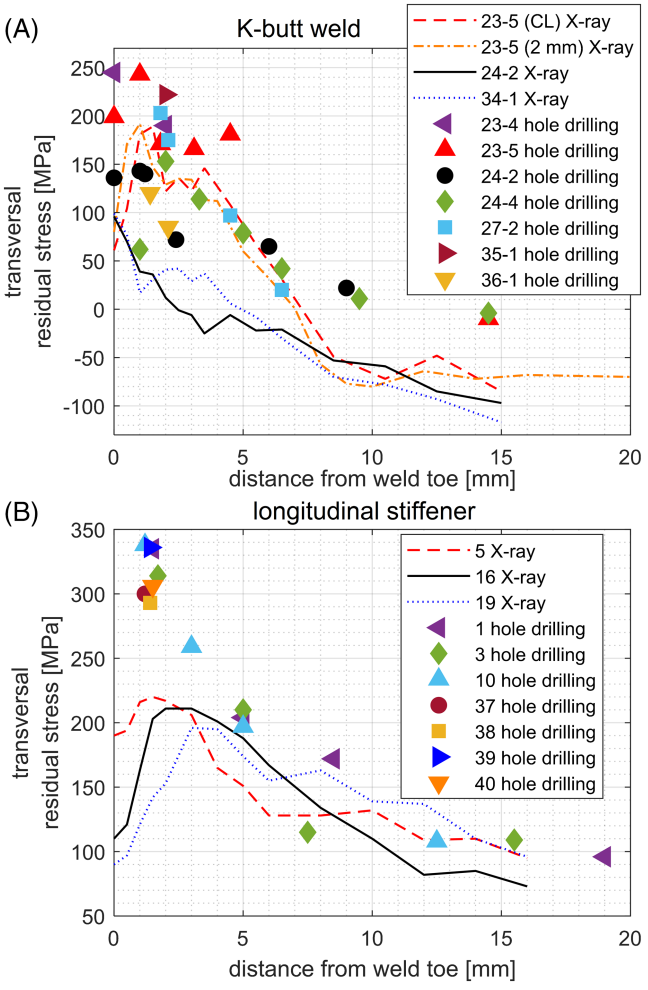

FIGURE 2 Transversal residual stress measured by hole drilling and X-ray diffraction on (A) K-butt weld specimens (referenced by the plate number XX and the position of the specimen 1–5 according to Figure 1) and (B) longitudinal stiffener specimens [Colour figure can be viewed at wileyonlinelibrary.com]

as it cools to room temperature resulting in a weld that is 'too short' compared with the surrounding material. Because this applies to the entire length of the weld, residual stresses will be present also in the specimens after cutting.

The residual stress measurements show tensile residual stresses transversal to the weld for both specimen geometries. In general, the hole drilling measurements resulted in higher values than the X-ray diffraction measurements. However, values from both measuring methods are not directly comparable, because residual stresses are measured at different depths. Using X-ray diffraction, the measurement depth is approximately 5 μm. The hole-drilling measurements are evaluated according to ASTM E837-13[20] assuming uniform stresses up 1-mm depth. Residual stresses were also measured on stress-relieved specimens of both types. The results, not included in the paper, show a clear reduction of the residual stresses and values close to zero at the weld toe.

Additional information on the residual stress measurements can be found in Friedrich and Ehlers.[15,16]

3 | FATIGUE TESTS

Fatigue tests are performed on both specimen geometries. The tests will reveal the residual stress influence on fatigue and show possible differences between the two weld geometries. Furthermore, in the tests, the residual stress influence on the initiation of macroscopic cracks and crack propagation will be studied, as there may be differences due to the non-uniform residual stress distribution over the thickness and different crack initiation to propagation ratios.

K-butt weld and longitudinal stiffener specimens are tested in as-welded and stress-relieved conditions. The residual stress influence depends on the applied load ratio. Tensile residual stresses will be more effective at low load ratios than at higher load ratios where the mean stress is already tensile. Therefore, four different load ratios R are applied in the tests. In all tests, the number of load cycles until initiation of a macroscopic crack is determined using DIC. For each test series, approximately 10 specimens are tested at different load ranges to establish the S-N curves.

To bring to light the influence of residual stresses, other influencing factors have to be minimised. In particular, the specimen distortion is critical. When the specimens are clamped, the secondary bending moments will generate stresses in the specimen that act as mean stresses. This would cover up the effect of the residual stresses. During specimen production, action was taken to minimise welding distortions. In the fatigue tests, levelling plates will be used when clamping the specimens to avoid the mean stress alteration due to clamping stresses.

3.1 | Test setup

The tests are performed on a 200-kN resonance testing machine. The specimen is clamped using hydraulic grips. For the DIC measurements, an ARAMIS 5M system is used with two cameras installed over the specimen. The DIC system serves two main purposes in the tests: first, to detect the initiation of macroscopic cracks and monitor crack propagation. Second, to measure strains caused by the clamping in order to reduce them using levelling plates.

3.2 | Clamping with levelling plates

When clamping the specimens in the testing machine, the angular distortion of the specimens causes a bending moment in the specimen. The resulting bending stresses act already before the actual load is applied and lead to a shift of the effective mean stress. In order to reduce these clamping stresses, shimming is applied by inserting levelling plates on top or underneath the specimen in the hydraulic grip at one end of the specimen. The plates have thicknesses between 0.2 and 5.6 mm. The required thickness is determined iteratively by measuring the strain at the weld using DIC. First, the specimen is clamped without any levelling plate, and strains are measured. On a distorted specimen, the strain will be either positive or negative depending on the direction of the distortion. The grip at one end of the specimen is reopened, and an appropriate levelling plate is put under or on top of the specimen's end, depending on the direction of the distortion. The grip is closed again, and strains are measured. This procedure is repeated until the measured strain is close zero.

To verify the effectiveness of the procedure, a K-butt weld specimen is equipped with strain gauges on the top and bottom side. The strain gauges are placed on the centre line of the specimen about 20 mm from the weld toe on the 10 mm plate. The specimen is clamped, and the DIC measurements are used to select the levelling plate. Clamping without levelling plate causes bending strains of about 0.011%, measured by both strain gauges and DIC. After inserting a levelling plate of 1.2 mm, the DIC results are close to zero. Strains measured by the strain gauges are 0.001%, corresponding to a bending stress of 2 MPa. This is acceptable small compared with the applied test loads and the accuracy of the involved equipment.

With the applied shimming procedure, clamping stresses are reduced. These would change the effective stress ratio at the weld and thus cover the influence of the residual stresses. The specimen distortion will induce bending stresses. But these are proportional to the applied load and will not change the stress ratio.

3.3 | Stopping criterion for $R = -\infty$

The tests are run until complete rupture of the specimen. Under compressive loading ($R = -\infty$), although the crack has divided the specimen, it will not break because the applied load presses the parts together. In some cases, the specimen is already completely divided, but the test will continue running. Thus, a different failure criterion has to be adopted.

On resonance testing machines, as the crack expands, it reduces the stiffness of the specimen and thus also the resonance frequency of the system. Usually, the moment when the specimen breaks is signed by a sudden decrease of the frequency (blue curve $R = 0$ in Figure 3). For $R = -\infty$, the loading frequency decreases slowly as the crack propagates and then stabilises at a certain frequency (red curve in Figure 3). At this point, the crack has almost reached the whole specimen cross-section and grows only very slowly. The value at which the frequency stabilises depends on the applied load and is therefore different for each test. These tests with $R = -\infty$ are stopped manually after the loading frequency has dropped and stabilised. The number of load cycles until failure is then determined at the point where the frequency has reached its final value (e.g., $N = 2.6{\cdot}10^6$ in Figure 3).

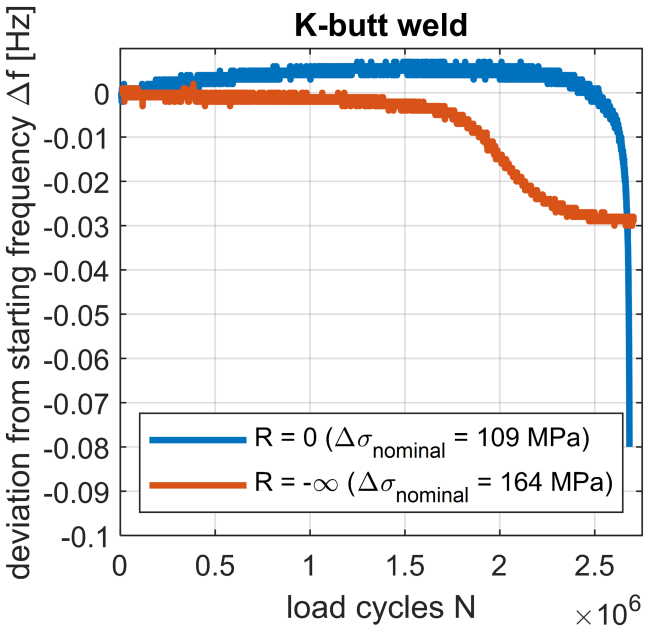

FIGURE 3 Development of the loading frequency during tests with tensile ($R = 0$) and compressive ($R = -\infty$) loading on K-butt weld specimens [Colour figure can be viewed at wileyonlinelibrary.com]

3.4 | Crack monitoring using DIC

To detect the initiation of macroscopic cracks, a procedure using DIC is adopted. It consists in measuring strains at the weld during the fatigue tests. Cracks will become visible as elevated strains in the loading direction of the specimen. To define the threshold value of strain indicating a crack, the DIC measurements are compared with beach marks introduced in fatigue tests with both specimen geometries. A value of 1% strain measured by DIC showed good agreement with the surface lengths of the beach marks. This value is in accordance with literature values in Kovárík et al.[21] For the tests, the initiation of a macroscopic crack is defined when the strains exceed a value of 1% over a length of 2 mm. This length could reliably be detected in the performed fatigue tests. Moreover, crack lengths of this magnitude can also be detected by more conventional means, for example, dye penetration testing and visual inspection, and may therefore be assumed as the initiation of macroscopic cracks from an engineer point of view. The initiation of a macroscopic crack on a K-butt weld specimen is exemplarily shown in Figure 4. The cameras for the DIC are triggered automatically by the load signal from the testing machine when the maximum load is applied and without interrupting the test. Images are acquired with an interval of load cycles to obtain about 100 or more images over the duration of the test. Detailed information on the applied DIC procedure can be found in Friedrich and Ehlers.[22]

4 | FATIGUE TEST RESULTS

Fatigue tests have been conducted on the K-butt weld and longitudinal stiffener specimens, in as-welded andstress-relieved conditions. The initiation of macroscopic cracks was detected by DIC. Hence, for each load ratio R, three S-N curves were established: for total fatigue life, for initiation of macroscopic cracks and for crack propagation. The S-N curves refer to the nominal stress range calculated by dividing the applied force range by the cross-section of the specimen.

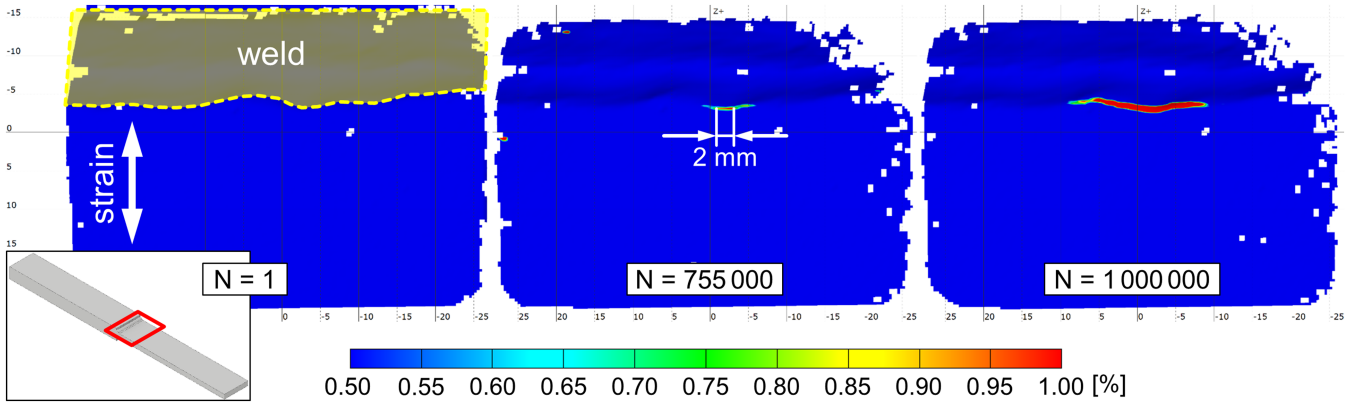

FIGURE 4 Percent strain in the loading direction on the first, static load cycle ($N = 1$) and at the initiation of a macroscopic crack on a K-butt weld specimen [Colour figure can be viewed at wileyonlinelibrary.com]

4.1 | K-butt weld

The resulting S-N curves for total fatigue life until complete rupture of the specimens are shown in Figure 5. The S-N curves are fit to the test results by linear regression. In the as-welded condition, the curves for $R = 0$ and $R = -1$ are close together. The results for $R = -3$ lie about 30% higher. All three curves have a slope exponent of approximately 3, which is the usual value for welded details. The curve for $R = -\infty$ is considerably steeper and differs from the others. In contrast, for the stress-relieved specimens, the curves for the different load ratios lie far away from each other. The curve for $R = 0$ is similar to the as-welded condition with a slightly shallower slope. For $R = -1$ and $R = -3$, the curves run much higher and have a slope exponent $k > 5$. For $R = -\infty$, only a run-out was produced, although the applied load was relatively high (309 MPa).

The S-N curve for FAT 71, which would apply for this type of weld according to the IIW recommendations,[23] is plotted as reference.

4.1.1 | Crack initiation

The initiation of macroscopic cracks was assessed by DIC. Crack initiation was determined when strains of 1% over a length of 2 mm could be detected. The resulting S-N curves for crack initiation are shown in Figure 6. The number of plotted results is smaller than in Figure 5 because it was not possible to determine crack initiation for all tested specimens. In some tests, the DIC system failed. In others, mostly with low load ratios ($R = -3$ or $R = -\infty$) cracks initiated on the bottom side of the specimen not covered by DIC. The distribution of the results is similar to the S-N diagrams for total fatigue life in Figure 5. In as-welded conditions, the curves for $R = 0$ and $R = -1$ are close together with a slope of approximately 3. The results for $R = -3$ lie slightly higher. For $R = -\infty$, the slope is again steeper. For the stress-relieved specimens, the distance between the S-N curves is

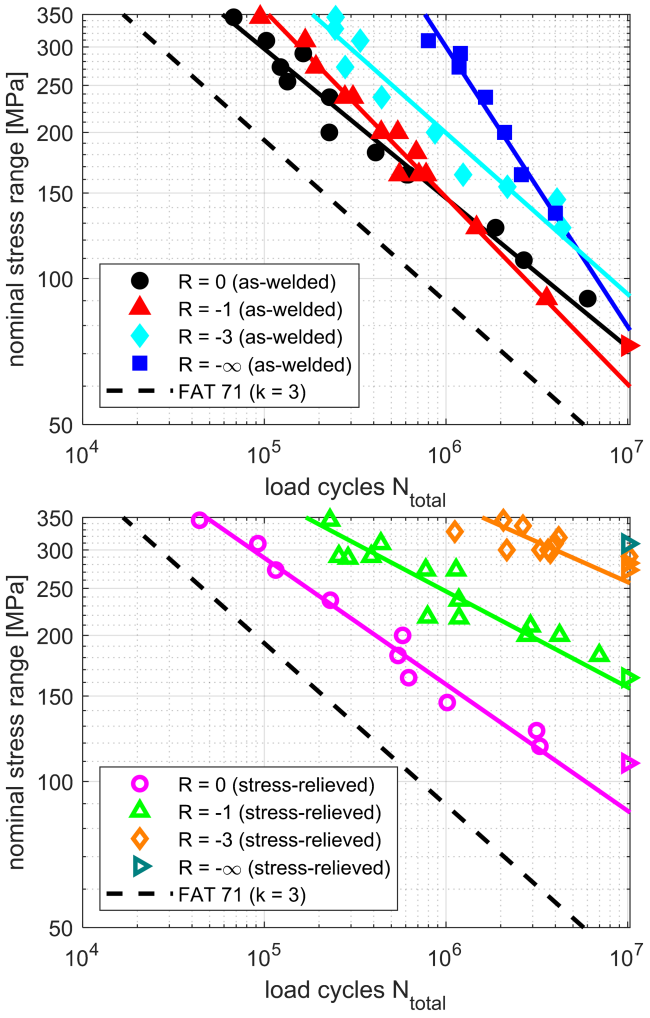

FIGURE 5 S-N curves for total fatigue life of as-welded (top) and stress-relieved (bottom) K-butt weld specimens (▶ symbol for run-out) [Colour figure can be viewed at wileyonlinelibrary.com]

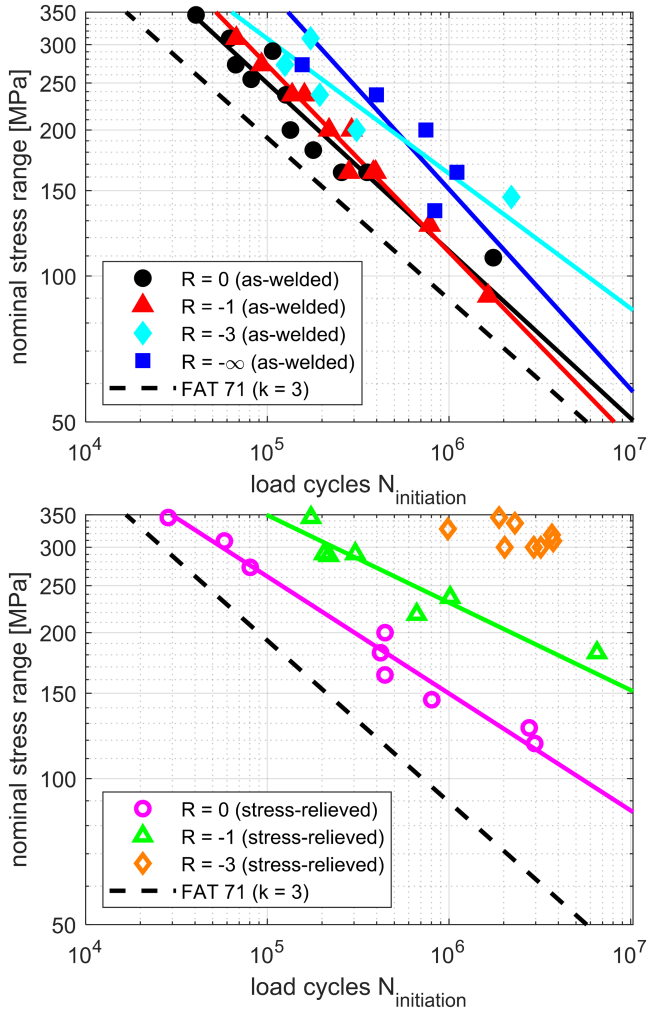

FIGURE 6 S-N curves for crack initiation for as-welded (top) and stress-relieved (bottom) K-butt weld specimens [Colour figure can be viewed at wileyonlinelibrary.com]

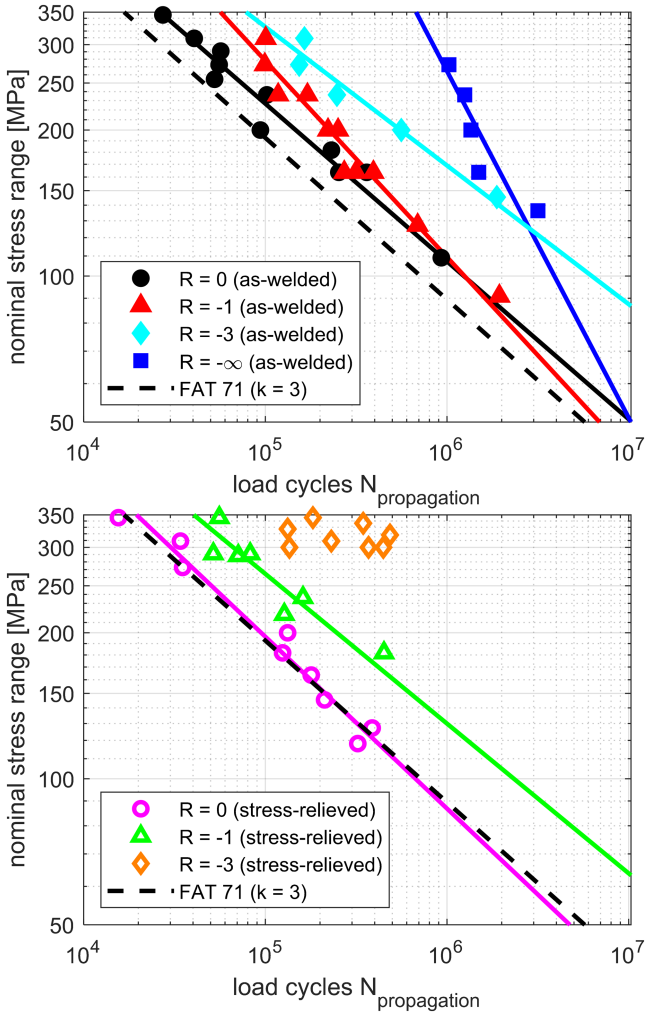

FIGURE 7 S-N curves for crack propagation for as-welded (top) and stress-relieved (bottom) K-butt weld specimens [Colour figure can be viewed at wileyonlinelibrary.com]

larger, and the slopes are shallower. For $R = 0$, at high load ranges, the results are similar to the as-welded condition. For low load ranges, the stress-relieved specimens show longer crack initiation periods, and the S-N curve has a shallower slope than in the as-welded condition. For $R = -3$, the results lie too close together to determine a representative S-N curve by linear regression.

4.1.2 | Crack propagation

The crack propagation phase is determined by subtracting the crack initiation from the total number of load cycles until rupture:

$$N_{propagation} = N_{total} - N_{initiation}. \quad (1)$$

The resulting S-N curves are plotted in Figure 7. In the as-welded condition, the curves are in the same range of the crack initiation curves, indicating a similar proportion of crack initiation and propagation on the total fatigue life. For the stress-relieved specimens, the crack propagation periods are shorter than the crack initiation, and the difference between the load ratios is less pronounced. In fact, the stress-relieved results lie close to the as-welded curves for the corresponding load ratio. For $R = -3$, in stress-relieved conditions, cracks did occur only for relatively high loads. The results lie too close together to determine a representative S-N curve by linear regression. The smaller numbers of load cycles ($N_{propagation} \approx 2{\cdot}10^5$) are close to the as-welded results.

4.1.3 | Discussion

The presented fatigue test results are influenced by welding residual stresses. In the as-welded condition, the

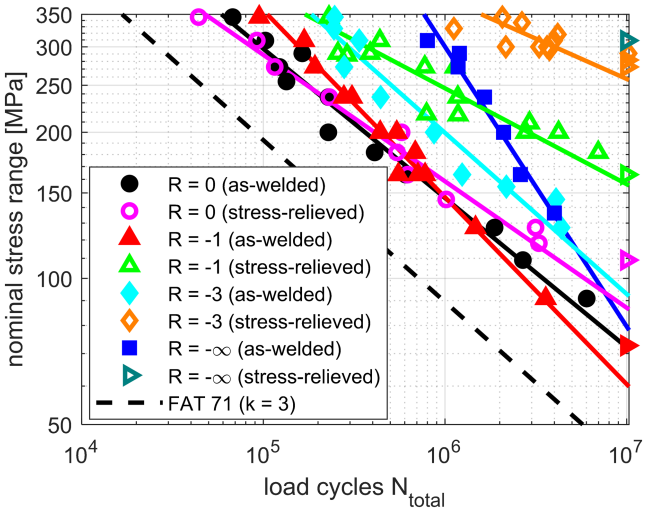

FIGURE 8 S-N curves for total fatigue life for as-welded and stress-relieved K-butt weld specimens (▶ symbol for run-out) [Colour figure can be viewed at wileyonlinelibrary.com]

S-N curves lie relatively close together because the tensile residual stresses reduce the influence of the load ratio. In the stress-relieved condition, the influence of the load ratio is more pronounced. By plotting all results in one S-N diagram, it becomes visible that the residual stress influence is more evident for lower load ratios (Figure 8). For tensile loading ($R = 0$), the results in as-welded and stress-relieved conditions are similar. With increasing compressive loads ($R = -1$ and $R = -3$), also the difference between as-welded and stress-relieved increases.

By plotting all results together, it becomes also visible that the S-N curves have different slopes. The slope can be interpreted as the increase of the damaging effect with an increase of the stress range. If by increasing the stress range the damaging effect increases rapidly, the endurable number of load cycles decreases faster, and the slope of the S-N curve is shallower. If with increasing stress range the damage increases slowly, the reduction of endurable load cycles is slow, and the S-N curve steep.

The S-N curves for total fatigue life (Figure 5) and for crack initiation (Figure 6) show a clear difference between as-welded and stress-relieved specimens. Crack propagation seems to be less affected by residual stresses (Figure 7). For each load ratio, the results from both residual stress conditions lie relatively close together. This indicates that residual stresses have little effect on the duration of crack propagation.

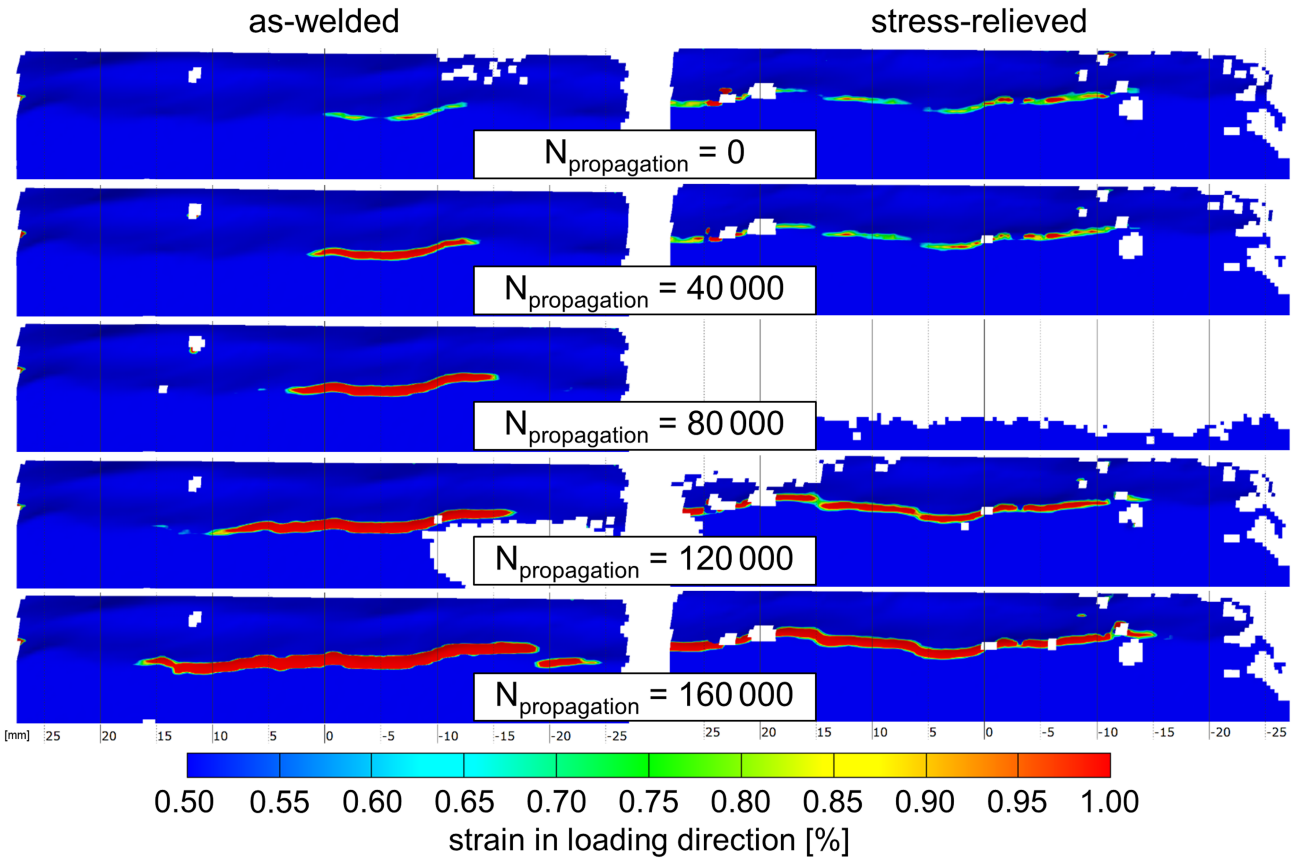

FIGURE 9 Crack propagation determined by DIC on an as-welded and a stress-relieved K-butt weld specimen ($R = -3$, nominal stress range = 309 MPa) [Colour figure can be viewed at wileyonlinelibrary.com]

Although the duration of crack propagation is similar on the as-welded and stress-relieved specimens, the development of cracks is different. On as-welded specimens, typically, a single crack was observed, whereas on stress-relieved specimens, often multiple cracks formed. Crack propagation detected by DIC for the same load range on an as-welded and a stress-relieved specimen is compared in Figure 9. On the as-welded specimen, a single crack forms close to the centre of the specimen and expands to both sides. On the stress-relieved specimen, several cracks form over the length of the weld. The cracks unify, and in the end, the resulting duration of crack propagation is similar to the as-welded specimen. This observation might be coincidental for this particular specimen geometry and residual stress distribution. Further investigations including crack propagation analysis would be necessary to determine why the crack propagation phases are similar for specimens with single and multiple cracks.

4.2 | Longitudinal stiffener

The S-N curves for total fatigue life until complete rupture of the longitudinal stiffener specimens are plotted in Figure 10. The design curve for this weld geometry is again FAT 71 according to the IIW recommendations,[23] and it is plotted as reference. In the as-welded condition, the curves for $R = 0$ and $R = -1$ lie close together and have the same slope. For $R = -3$, the curve is close to the first two curves up to 200 MPa. For higher load ranges, the number of endurable load cycles stays constant, and the S-N curve rises vertically. For compressive loads ($R = -\infty$), failures are observed only between 160 and 195 MPa. For lower and higher load ranges, only

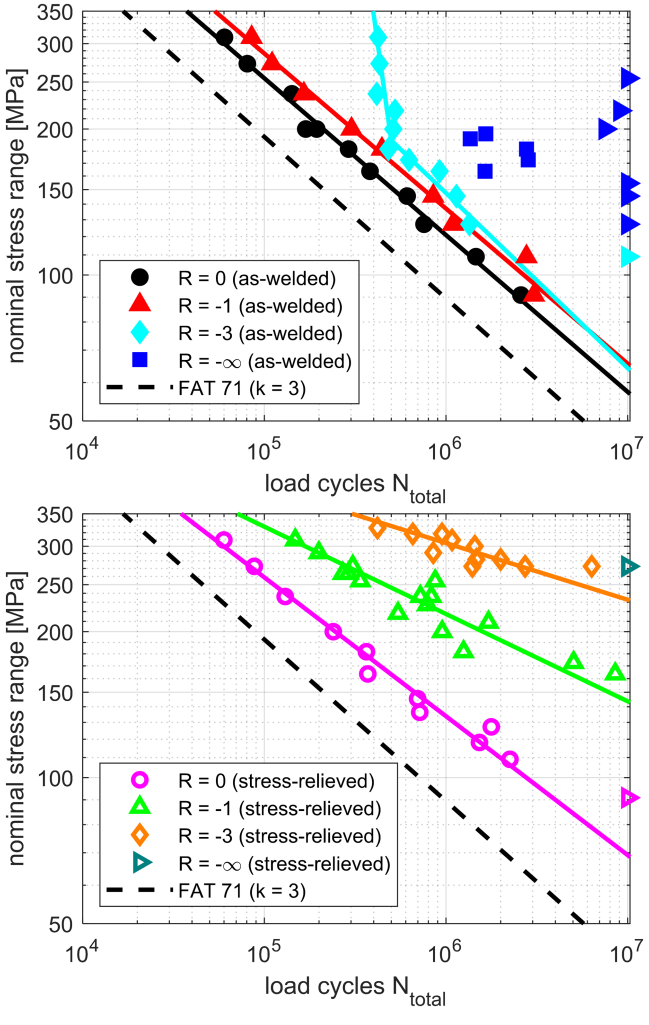

FIGURE 10 S-N curves for total fatigue life of as-welded (top) and stress-relieved (bottom) longitudinal stiffener specimens (▶ symbol for run-out) [Colour figure can be viewed at wileyonlinelibrary.com]

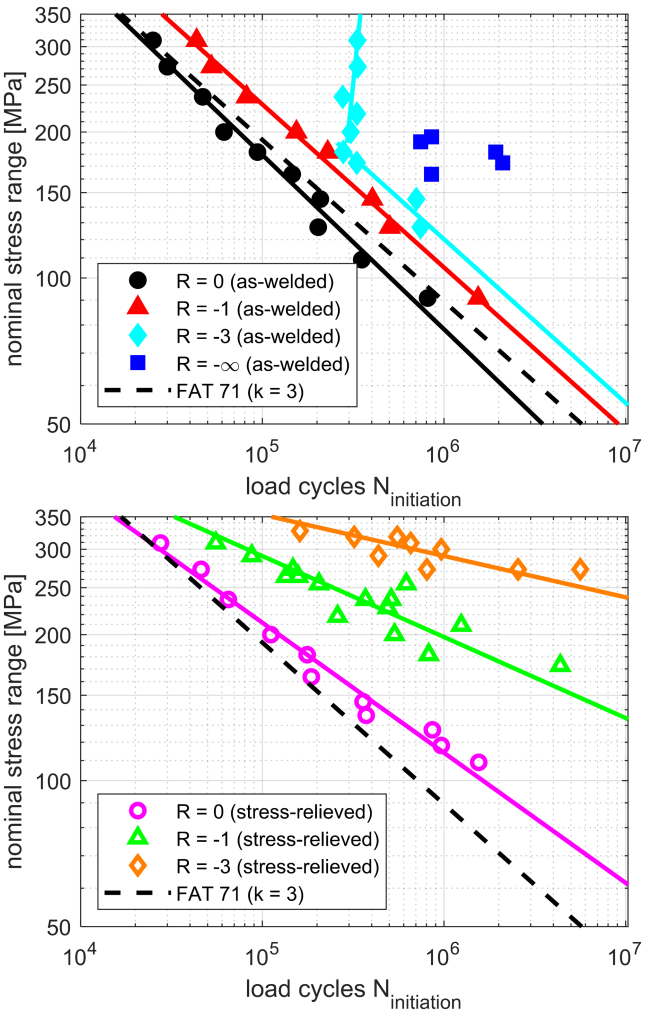

FIGURE 11 S-N curves for crack initiation for as-welded (top) and stress-relieved (bottom) longitudinal stiffener specimens [Colour figure can be viewed at wileyonlinelibrary.com]

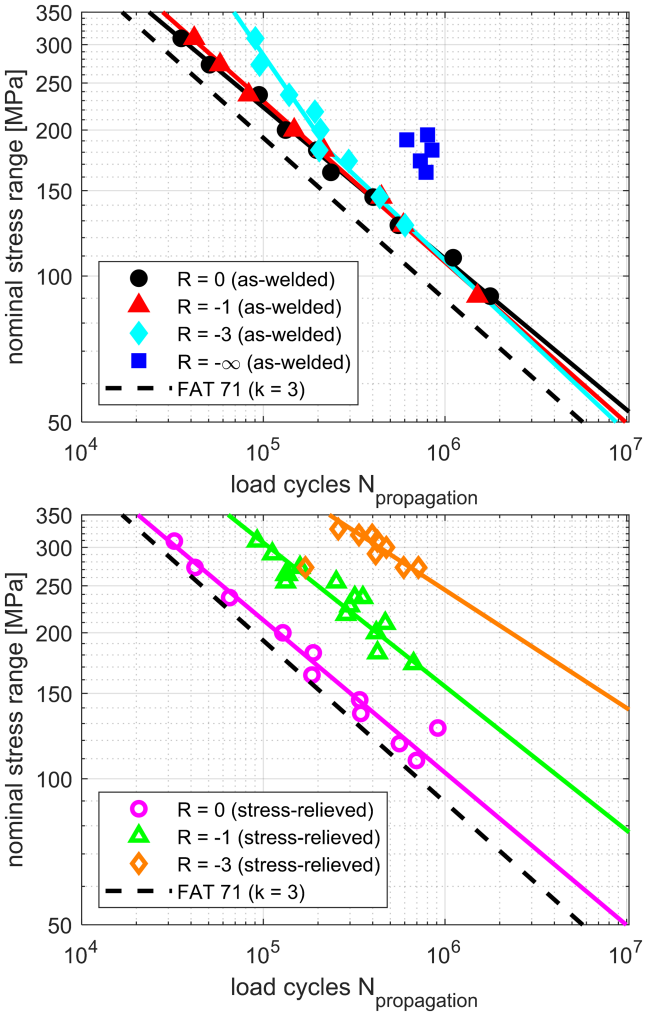

FIGURE 12 S-N curves for crack propagation for as-welded (top) and stress-relieved (bottom) longitudinal stiffener specimens [result for $R = -3$ (stress-relieved) at $N_{propagation} = 1.7 \cdot 10^5$ not included in linear regression] [Colour figure can be viewed at wileyonlinelibrary.com]

run-outs were obtained. The stress-relieved curves clearly show the influence of the different load ratios. Except for tensile loads ($R = 0$), the curves run higher than the as-welded curves and have a shallower slope. For compressive loads ($R = -\infty$), only a run-out was produced.

4.2.1 | Crack initiation

The S-N curves for the initiation of macroscopic cracks are shown in Figure 11. The results for the as-welded specimens are qualitatively similar to the previous curves for total fatigue life. The curves for $R = 0$ and $R = -1$ lie close together. For $R = -3$, the curve runs vertical above 200 MPa. For $R = -\infty$, cracks were detected only between 160 and 195 MPa. For the stress-relieved specimens, the influence of the different load ratios is clearly visible. The curves run higher and with a shallower slope than in the as-welded condition.

4.2.2 | Crack propagation

The number of load cycles for crack propagation is calculated by subtracting the number of load cycles until initiation of a macroscopic crack from the total number of load cycles. The resulting S-N curves are shown in Figure 12. For the as-welded specimens, the curves for load ratios from $R = 0$ to $R = -3$ overlap. Thus, no influence of the load ratio is apparent. For compressive loads ($R = -\infty$), the results lie close together and higher than for the other three load ratios. The stress-relieved specimens show clear differences for the different load ratios. For tensile loads ($R = 0$), the crack propagation phase is slightly shorter than in the as-welded condition. For

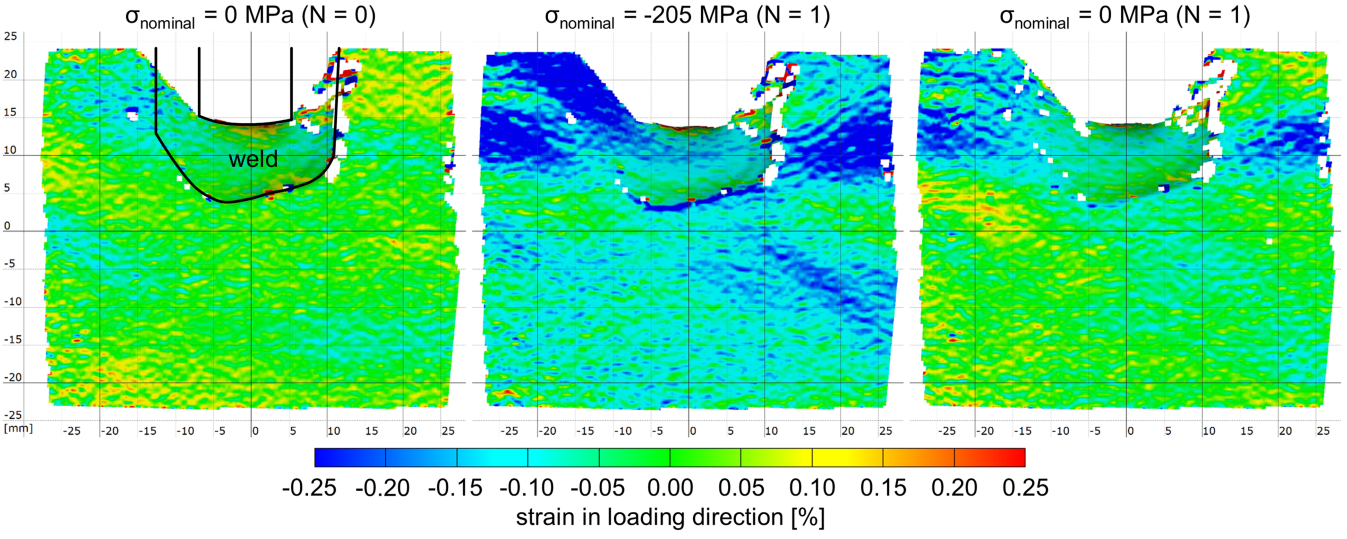

FIGURE 13 Strain measured by digital image correlation (DIC) at the end of the longitudinal stiffener before, during and after applying a compressive load [Colour figure can be viewed at wileyonlinelibrary.com]

$R = -1$ and $R = -3$, the curves lie considerably higher than for the as-welded specimens.

4.2.3 | Discussion

Also the fatigue test, results for the longitudinal stiffeners show a clear influence by residual stresses. Remarkable are the tests in as-welded condition for low load ratios, $R = -\infty$ and $R = -3$, which resulted in non-linear S-N curves (Figure 10). Strains measured by DIC before, during and after applying a compressive load are plotted in Figure 13. Under load, the highest compressive strains occur at the weld toe and to the sides of the stiffener. After unloading, compressive strains persist on the sides of the stiffener. Also at the weld toe, strains remain compressive. From the DIC measurements, it cannot be determined whether these are plastic strains or elastic strains caused by the surrounding compressive field. Elastic compressive strains would reduce the tensile

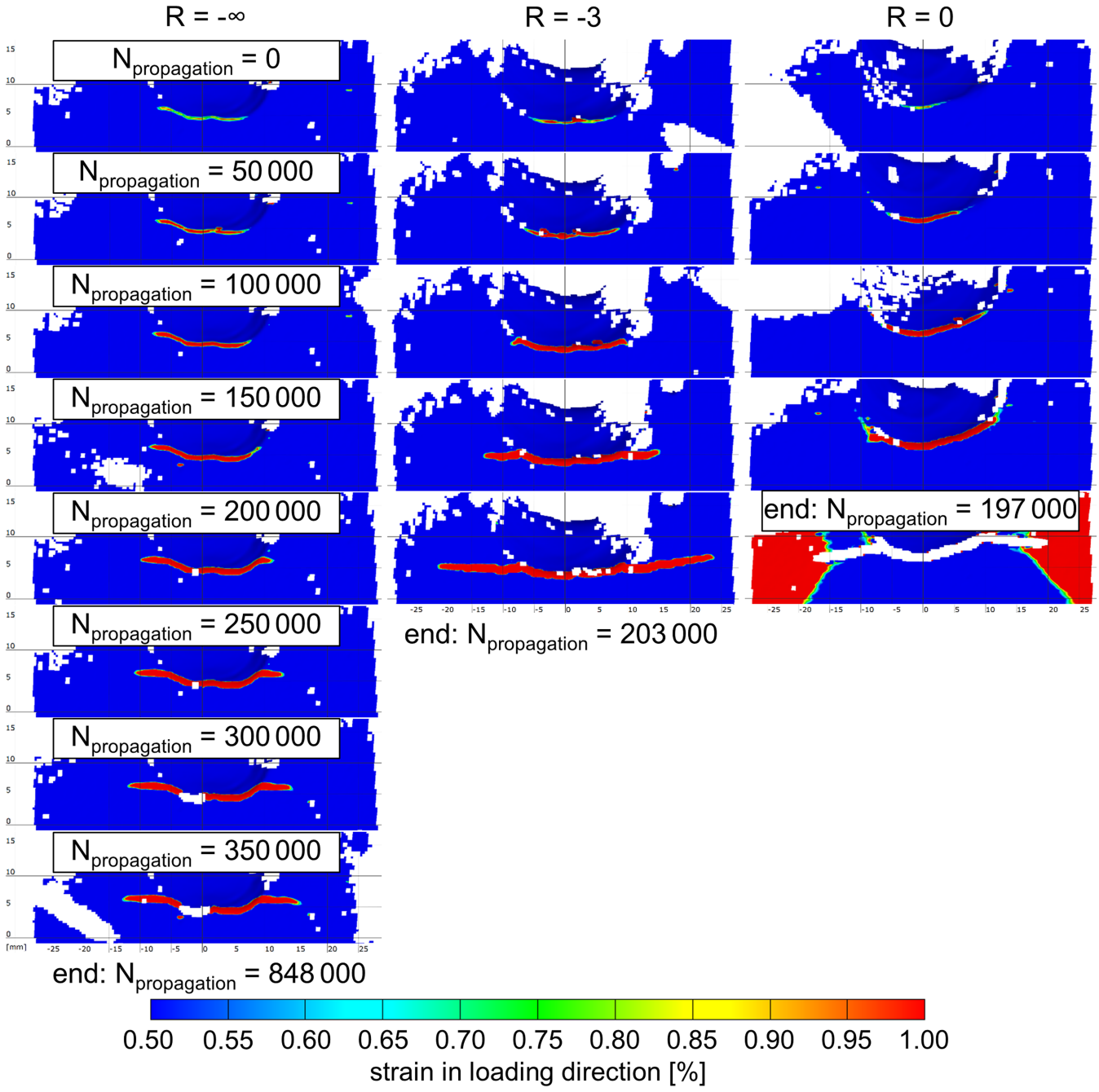

FIGURE 14 Crack propagation determined by digital image correlation (DIC) on as-welded specimens tested with different load ratios R (nominal stress range = 182 MPa) [Colour figure can be viewed at wileyonlinelibrary.com]

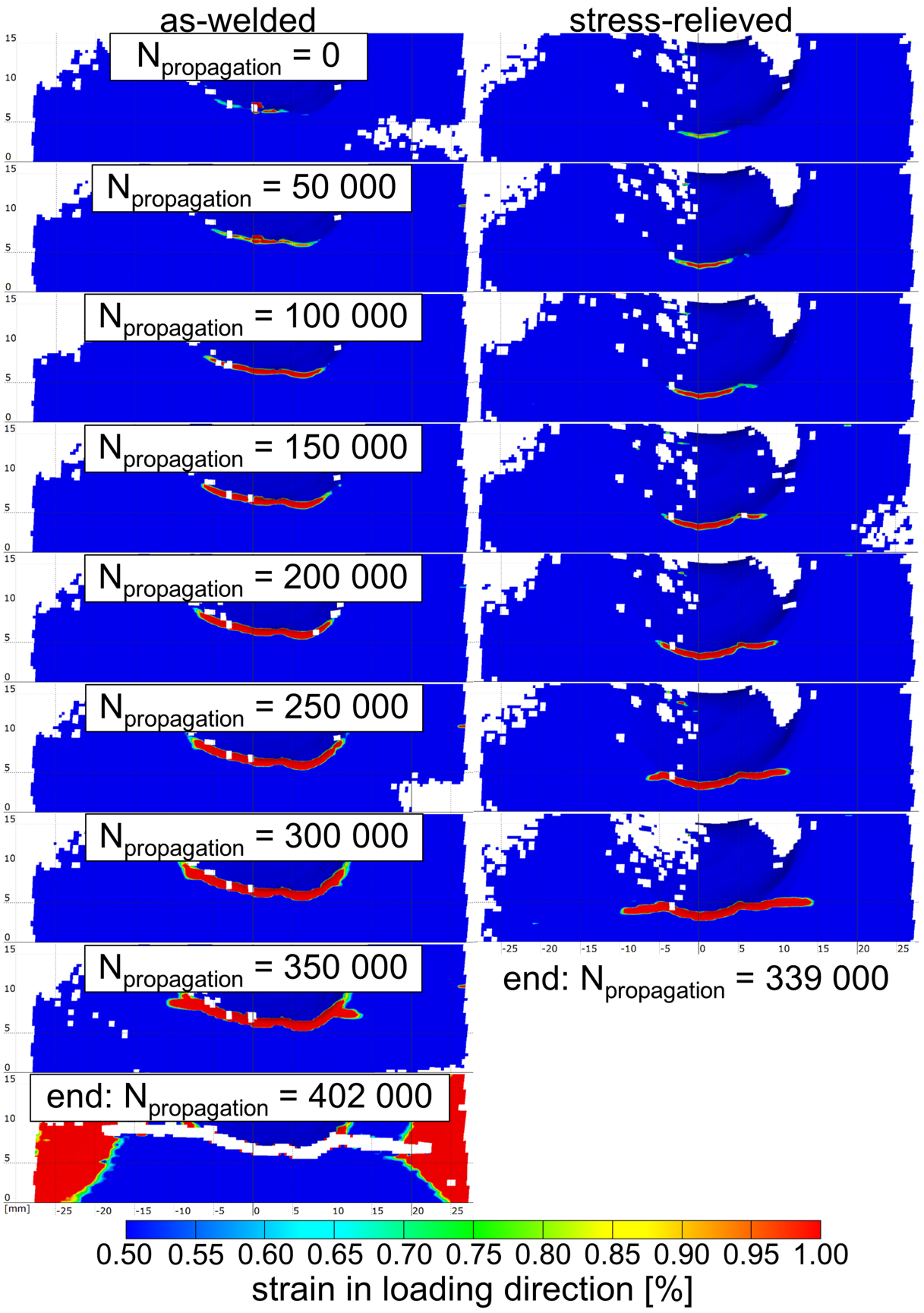

FIGURE 15 Crack propagation determined by digital image correlation (DIC) on an as-welded and a stress-relieved specimen under tensile loading $R = 0$ (nominal stress range = 145 MPa) [Colour figure can be viewed at wileyonlinelibrary.com]

residual stresses at the weld toe. Plastic compressive strains could cause tensile residual stresses themselves. These results indicate that fatigue test results under compressive loads are influenced by a redistribution of residual stresses due to plastic strains in the cross-section of the specimen.

Stresses at the weld toe will influence crack initiation. But the residual stress influence is also visible in the S-N diagram for crack propagation (Figure 12). For the stress-relieved specimens, the influence of the load ratio is clearly visible. In the as-welded condition, crack propagation seems to be independent of the applied load ratio, with exception of compressive loads ($R = -\infty$). Crack lengths measured on as-welded specimens tested with load ratios of $R = 0$, $R = -3$ and $R = -\infty$ at the same nominal stress range are compared in Figure 14. For $R = 0$ and $R = -3$, the development of the crack is similar. For compressive loads ($R = -\infty$), the crack length visible on the surface is initially comparable, as long as the crack grows in front of the weld ($N_{propagation} < 150\ 000$). As it extends into the girder, crack propagation is slower than for the other two load ratios.

Despite the fact that crack growth is accelerated by tensile residual stresses, from the S-N diagram (Figure 12), it appears that the fastest crack growth is achieved on stress-relieved specimens with tensile loading ($R = 0$). This S-N curve runs even lower than in the as-welded condition. A reason could be the slightly higher distortions of the stress-relieved specimens, but the distortion would affect also crack initiation. From the DIC measurements, it appears that the crack development is different for the as-welded and the stress-relieved specimens. Exemplarily, the crack development for a nominal stress range of 145 MPa at $R = 0$ is shown in Figure 15. On the as-welded specimen, the crack grows quickly to a length of about 18 mm at which it covers the entire front of the weld. Then, the crack length increases only slowly, and the crack tip stays at the weld toe, before leaving the weld and advancing into the girder ($N_{propagation} > 300\ 000$). On the stress-relieved specimen, initially, the crack grows slower, but it proceeds steadily from the weld into the girder. In the end the crack propagation phase is shorter than on the as-welded specimen. A similar development of the crack length was observed also on other specimens tested at different stress ranges and a load ratio of $R = 0$.

5 | CONCLUSIONS

The influence of welding residual stresses on fatigue was investigated in experimental tests on multilayer K-butt weld and longitudinal stiffener specimens. Residual stresses were determined by X-ray diffraction and hole drilling. Fatigue tests at different load ratios were conducted on specimens in as-welded and stress-relieved conditions. Besides the total fatigue life, the initiation of macroscopic cracks and the following crack propagation was detected using DIC.

On both specimen geometries, tensile residual stresses were determined at and in front of the weld. On the K-butt weld, this was achieved by applying a specific welding sequence.

On both specimen geometries, fatigue test results for total fatigue life were influenced by the residual stresses. In the as-welded condition, the influence of the load ratio R was small compared with the stress-relieved specimens. The latter resulted in higher numbers of load cycles N and S-N curves with shallower slopes. These differences increased for lower load ratio, that is, more compressive loads. For purely compressive loads ($R = -\infty$), failures were observed only in the as-welded condition.

A similar residual stress influence was observed in the number of load cycles until initiation of a macroscopic crack. In as-welded conditions, the influence of the load ratio was reduced compared with the stress-relieved condition for both specimen geometries.

The duration of crack propagation was affected differently on both specimen types. On the K-butt weld, the observed duration of crack propagation was similar for as-welded and for stress-relieved specimens. However, the form of the cracks was different. In the as-welded specimens, typically, a single crack initiated at the centre of the specimen and propagated to both sides. In the stress-relieved specimens, often multiple cracks formed over the length of the weld and eventually unified. Further investigations are necessary to clarify if the similar duration of the crack propagation phase for specimens with single and multiple cracks is coincidental for this particular specimen geometry.

On the longitudinal stiffeners, also crack propagation was influenced by the residual stresses. This influence showed in the duration of crack propagation and in different crack development in vicinity of the weld and in the girder.

Overall, the residual stress influence on total fatigue life was predominantly determined by the initiation of macroscopic cracks. However, the latter was determined at a length of 2 mm, which is relatively long.

ACKNOWLEDGEMENTS

The presented research was funded by the Deutsche Forschungsgemeinschaft (DFG, German Research Foundation) – EH 485/4-1. The author thanks Prof Sören Ehlers for the support in this project. Open access funding enabled and organized by Projekt DEAL.

NOMENCLATURE

ASTM	American Society for Testing and Materials
CL	Centre Line
DIC	Digital Image Correlation
IIW	International Institute of Welding
k	slope exponent according to the *Basquin* equation: $N = N_R \left(\frac{\Delta\sigma}{\Delta\sigma_R}\right)^{-k}$
N	endurable number of load cycles
N_{total}, $N_{initiation}$, $N_{propagation}$	endurable number of load cycles for total fatigue life, crack initiation and propagation
N_R	reference number of load cycles = $2 \cdot 10^6$
R	load ratio $\sigma_{nominal,min}/\sigma_{nominal,max}$
R_{eH}	upper yield strength
$R_{p0.2}$	yield strength at 0.2% plastic strain
Δf	deviation from loading frequency at the start of the test
$\Delta\sigma$	stress range
$\Delta\sigma_R$	reference stress range at $N_R = 2 \cdot 10^6$

ORCID

Nils Friedrich https://orcid.org/0000-0002-2250-3819

REFERENCES

1. Gurney TR. *Fatigue of Welded Structures*. 2nd ed. UK: Cambridge University Press; 1979.
2. Nitschke-Pagel T. *Eigenspannungen und Schwingfestigkeitsverhalten geschweißter Feinkornbaustähle [Residual Stresses and Fatigue Strength of Welded Fine Grained Steel, in German]*. Dissertation. Germany: TU-Braunschweig; 1995.
3. Buxbaum O. *Betriebsfestigkeit: Sichere und wirtschaftliche Bemessung schwingbruchgefährdeter Bauteile [Fatigue Strength: Safe and Economic Design of Fatigue-Prone Components, in German]*. Germany: Verlag Stahleisen; 1986.
4. Varfolomeev I, Moroz S, Brand M, Siegele D, Baumgartner J. *Lebensdauerbewertung von Schweißverbindungen unter besonderer Berücksichtigung von Eigenspannungen, Schlussbericht IGF-Vorhaben 15.913 N [Fatigue Assessment of Welds Under Consideration of Residual Stresses, in German]*. Germany: Fraunhofer IWM; 2011.
5. Siegele D, Baumgartner J, Varfolomeev I, Moroz S, Brand M, Bruder T. Lebensdauerbewertung von Schweißverbindungen unter besonderer Berücksichtigung von Eigenspannungen [Fatigue life assessment of welds under consideration of residual stresses, in German]. *Schweißen und Schneiden*. 2013; 65(3):128-135.
6. Hensel J, Nitschke-Pagel T, Dilger K. Effects of residual stresses and compressive mean stresses on the fatigue strength of longitudinal fillet-welded gussets. *Weld World*. 2016;60(2): 267-281.
7. Ferro P. The local strain energy density approach applied to pre-stressed components subjected to cyclic load. *Fatigue Fract Eng Mater Struct*. 2014;37(11):1268-1280.
8. Ferro P, Berto F. Quantification of the influence of residual stresses on fatigue strength of Al-alloy welded joints by means of the local strain density approach. *Strength Mater*. 2016;48(3): 426-436.
9. Bate SK, Green D, Buttle D. *A Review of Residual Stress Distributions in Welded Joints for the Defect Assessment of Offshore Structures*. Health and Safety Executive: UK; 1997.
10. Chattopadhyay A, Glinka G, El-Zein M, Qian J, Formas R. Stress analysis and fatigue of welded structures. *Weld World*. 2011;55(7-8):2-21.
11. Rörup J. *Einfluss von Druckmittelspannungen auf die Betriebsfestigkeit von geschweißten Schiffskonstruktionen [The Effect of Compression Mean Stresses on the Fatigue Strength of Welded Ship Structures, in German]*. Dissertation. Germany: Schriftenreihe Schiffbau Bericht; 2003:619.
12. Tateishi K, Takeshi H, Tsuruta Y, Sasadad S, Choi SM. Fatigue life extension of cracked welded joints by ICR treatment under tensile loading. *10th Pacific Structural Steel Conference*. Singapore; 2013.
13. Lepore M, Berto F, Maligno AR, Fellinger J. Nonlinear fatigue crack propagation in a baffle module of Wendelstein 7-X under cyclic bending loads. *Fatigue Fract Eng Mater Struct*. 2019; 42(8):1711-1721.
14. Lepore M, Maligno AR, Berto F. Crack closure in friction stir weldment using non-linear model for fatigue crack propagation. *Fatigue Fract Eng Mater Struct*. 2019;42(11): 2596-2608.
15. Friedrich N, Ehlers S. A simplified welding simulation approach used to design a fatigue test specimen containing residual stresses. *Ship Technol Res*. 2019;66(1):22-37.
16. Friedrich N, Ehlers S. Experimental validation of a simplified welding simulation approach for fatigue assessments. In: Sommitsch C, Enzinger N, Mayr P, eds. *Mathematical Modelling of Weld Phenomena 12*. Graz: Verlag d. Technischen Universität Graz; 2019:875-891.
17. Narazaki M, Totten GE. Distortion of heat-treated components. In: Totten GE, ed. *Steel Heat Treatment Handbook, Second Edition—Steel Heat Treatment: Metallurgy and Technologies*. Boca Raton: Taylor and Francis; 2007:607-650.
18. Fricke W, Lilienfeld-Toal A, Paetzold H. Versteifte Plattenstrukturen aus dem Stahlschiffbau im Cluster Anwendbarkeit von Festigkeitskonzepten für schwingbelastete geschweißte Bauteile, CMT 14/2009, AiF-Vorhaben 14517N [Stiffened plate structures in steel shipbuilding in the cluster of applicability of strength concepts for welded components under fatigue loads, in German]. Germany; 2009.
19. Fricke W, Tchuindjang D. Abschlussbericht zum AiF-Vorhaben 17519 N Rissfortschrittsuntersuchung an Längssteifen zur Validierung der IBESS-Prozedur [Report to the AiF-project 17519 N crack propagation investigations on longitudinal stiffeners for validation of the IBESS-procedure, in German]. Germany; 2016.
20. ASTM E837-13a. *Test Method for Determining Residual Stresses by the Hole-Drilling Strain-Gage Method*. ASTM International: West Conshohocken, PA; 2013.

21. Kovárík O, Haušild P, Medřický J, et al. Fatigue crack growth in bodies with thermally sprayed coating. *J Therm Spray Technol*. 2016;25(1–2):311-320.
22. Friedrich N, Ehlers S. Crack monitoring in resonance fatigue testing of welded specimens using digital image correlation. *J Vis Exp*. 2019;151:e60390. https://doi.org/10.3791/60390
23. Hobbacher AF. *Recommendations for Fatigue Design of Welded Joints and Components (IIW Collection; Second Edition)*. Switzerland: Springer; 2016.

How to cite this article: Friedrich N. Experimental investigation on the influence of welding residual stresses on fatigue for two different weld geometries. *Fatigue Fract Eng Mater Struct*. 2020;43:2715–2730. https://doi.org/10.1111/ffe.13339